SP-230—14

Out-of-Plane Static and Blast Resistance of Unreinforced Masonry Wall Connections Strengthened with FRP

by P. Carney and J.J. Myers

Synopsis: Recent world events have illustrated that the sustainability of buildings to blast loads is an ever increasing issue. Many older buildings contain unreinforced masonry (URM) infill walls. Due to their low flexural capacity and their brittle mode of failure, these walls have a low resistance to out-of-plane loads, which includes blast loads. As a result, an effort has been undertaken to examine retrofit methods that are feasible to enhance their out-of-plane resistance. The use of externally bonded and near surface mounted (NSM) Fiber Reinforced Polymer (FRP) laminates and rods have been proven to increase the out-of-plane load capacity.

This paper investigates the out-of-plane behavior of URM walls strengthened with FRP subjected to static and blast loading and the capability of developing continuity between the FRP strengthening material and the surrounding reinforced concrete (RC) frame system. There were two phases to this research study. Phase I evaluated strengthened URM walls' out-of-plane performance using static tests. Two strengthening methods were utilized, including the application of glass FRP (GFRP) laminates to the wall's surface and the installation of near surface mounted (NSM) GFRP rods. In both methods, the strengthening material was anchored to boundary members above and below the wall on some of the specimens in the research program. The effects of bond pattern, and the effects of FRP laminate strip width were also investigated in this phase. Phase II involved the field blast testing of two walls to dynamically study the continuity detail for laminates and verify the results obtained in Phase I. The development of continuity between the FRP materials and the surrounding framing system is one approach to improving the blast resistance of URM infill walls.

Keywords: blast resistance; FRP strengthening; masonry wall connections; masonry wall retrofits

ACI member **John J. Myers** is an Associate Professor at the University of Missouri-Rolla. He received his BAE from The Pennsylvania State University; MS and Ph.D. from University of Texas-Austin. His research interests include high performance concrete and use of fiber-reinforced polymers in structural repair and strengthening applications. He is a member of ACI Committees 201, 342, 363, 440, E801, E802, and E803. He is the current sub-committee co-chair of 440L (durability of FRP concrete structures) and chair of E801.

Preston Carney is a structural design engineer with Wallace Engineering Inc. located in Tulsa, Oklahoma. He has a BS and MS from the University of Missouri-Rolla in Civil Engineering.

INTRODUCTION

Recent events throughout the world have drawn attention to the vulnerability and sustainability of buildings and infrastructure to acts of terrorism. Our infrastructure is vital to this nation's economy and way of life. Any damage to it would and has had drastic effects on our culture. Attacks may cause a variety of results ranging from minor building damage to complete structural failure and considerable loss of life. Some examples within the United States include the bombing of the Murrah Federal Building in Oklahoma City (1995) and the bombing and attacks on the World Trade Center in New York City (1993, 2001). Abroad, numerous attacks have been directed toward embassies, and suicide car bombers have been used to target populated areas. In the cases where complete structural failure is not an issue, the dangers of flying debris have resulted in loss of life or injury to numerous civilians. Of particular concern are unreinforced masonry (URM) infill walls. Structural systems composed of a reinforced concrete (RC) framing system with URM infill walls make up a significant portion of the building inventory in the United States and around the world. Since there is no reinforcement within these walls, they have little resistance to out-of-plane loads such as a blast load. As a result, an effort has been undertaken to examine retrofit methods that are feasible to enhance their out-of-plane resistance. One method of strengthening URM walls is the application of fiber reinforced polymers (FRP) to the surface of the wall to improve their performance.

Since the effects of a blast cause a pressure to be exerted on the surface of a wall, the flexural behavior of the wall can be observed. This makes it appropriate to strengthen the walls to improve their flexural capacity. The application of externally bonded FRP materials have been shown to improve the flexural capacity of walls with and without arching action (El-Domiaty et al., 2002), but the development of continuity between the wall system and surrounding boundary members needs to be investigated.

Strengthening of walls is not the only step involved in the process of reducing a building's vulnerability to blast loadings. Proper risk assessment must also be performed to determine the level of vulnerability of a structure. One must also determine the level of damage that is acceptable for the structure to sustain. The characteristics of an explosion are key in assessing this vulnerability. The pressures that are developed as a result of an explosion are a function of the weight of the charge and the distance from the explosion, commonly called the standoff distance. The charge weight is expressed in terms of equivalent weight of trinitrotoluene (TNT). As the charge weight increases, the

pressures that are developed are also increased. Similarly, as the standoff decreases, the pressures on a surface increase. For a given charge weight, the effects may be drastically different if the standoff distance is changed. For a very small standoff distance, strengthening the wall per say may have little effect; rather the addition of significant mass in the form of thick walls is often the approach. However, it may be more appropriate to try to increase the standoff distance to a facility by implementing barriers or restricting vehicular access to a structure. Wall strengthening would then allow for a compromise, that is the standoff distance would only have to be increased to the point which the strengthened wall could withstand the pressure from the design blast. With the proper assessment and an understanding of the key parameters, the strengthening of URM infill walls with FRP to improve their blast resistance has great potential.

EXPERIMENTAL PROGRAM

This research program made use of two FRP composite strengthening systems. The systems were laminate manual lay-up and near surface mounted (NSM) rods. Both systems use E-glass based fibers.

Out-of-plane testing

The testing of URM walls in the out-of-plane direction can be accomplished in a variety of ways. Several different methods of loading have been utilized in previous research to effectively apply a static load. Some research programs have applied a point load either at center span or used a device to apply two point, or line, loads on either side of the midpoint of the wall. A complex, but effective method of applying a uniform load is the use of a pressurized water chamber. A wall can be constructed between two tanks and one of them pressurized to apply a uniform load to the wall. A simpler method is the use of an airbag which is what was used in Phase I of this study. An airbag can be used to apply a load by placing the bag in contact with the test wall and a reaction structure. The airbag used in this research program had deflated dimensions of 36 in (914.4 mm) wide by 48 in (1219.2 mm) tall. They were six ply paper dunnage bags commercially produced by International Paper's Ride Rite Division. They were capable of withstanding pressures of over 20 psi (138 kPa) based on testing by the manufacturer.

Test matrix

The development of this test program extended previous research performed at UMR (El-Domiaty et al., 2002). The previous work illustrated that strengthening masonry walls with FRP materials does in fact improve their out-of-plane performance. This research was conducted to further investigate the effectiveness of strengthening URM walls with several variables.

This study was completed in two phases. Phase I was the evaluation of the retrofit techniques under static loading conditions using an airbag to incrementally load the walls to failure. Phase I was divided into two series. Series I consisted of six test walls. Series II was composed of an additional six walls based on the results obtained from Series I. Phase II was the field evaluation of two walls under actual blast loading. The walls in both phases were constructed of 4 in x 8 in x 12 in (101.6mm x 203.2 mm x 304.8 mm) CMU. The overall dimensions of the walls were 48 in (1219.2 mm) tall by 36 in (914.4 mm) wide. These dimensions result in a slenderness ratio of 12. The slenderness ratio of a 10 ft (3.05 m) tall wall constructed out of 8 in (203.2 mm) thick blocks is

approximately 15. Therefore, the slenderness ratio used in this research program is comparable to what would be expected in an existing building. The 36 in (914.4 mm) wide dimension allowed for the wall to be three blocks wide giving two vertical, or head, joints in each wall. The FRP was applied along or within each of the head joints. It may be noted that 8 in (203.2 mm) thick walls were not tested due to limitations in the capacity of the air bags to meet the required failure pressure requirements of thicker wall units.

After Series I walls were tested, the test program for Series II was developed. Walls #1 and #2 served as unreinforced control walls in Phase I. Walls #7 and #8 in Series II served as strengthened FRP control walls without anchorage details. These were strengthened, but do not make use of the anchorage techniques. This allowed for a direct measure of the increase in capacity associated with the use of anchorage. The walls in Series I were all constructed using a stacked bond pattern. Since many facilities are constructed using a running, or staggered, bond, it was necessary to study the effects of bond pattern. This was done by constructing two of the walls (Walls #9 and #10) using a running bond. Both FRP retrofit techniques with anchorage were tested using this bond pattern. Series II concluded by studying the effects of the reinforcement ratio, or the width of the laminate strip. The final two walls made use of laminate strips that were 4.5 in (114.3 mm) and 6.5 in (165.1 mm) wide to investigate how the capacity of the walls changes as the amount of reinforcement on the walls increases. This change is only possible when using the laminates. The amount of reinforcement in the case of NSM bars cannot be increased without cutting additional grooves in the blocks due to the size limitations of the mortar joints.

The research program concluded with Phase II. This was the field blast testing of two walls. Under static loading, the laminates performed better than the NSM rods, so they were selected for use in this phase to evaluate their performance under short dynamic (blast) loading. One wall made use of 2.5 in (63.5 mm) laminates unanchored, while the other wall had the same reinforcement, but the FRP was anchored to the boundary members and the shear retrofit was included.

This experimental program investigated the development of continuity between the FRP and the boundary members. Several other variables were also examined, including the effects of bond pattern, and the effects of the width of the laminate strips. The test program is summarized in Table 1. Two FRP strengthening methods were utilized in this research along with anchorage techniques for both methods. The first strengthening technique is the use of externally bonded glass FRP laminates as shown in Figure 1. The laminates (fabrics) are applied vertically to the surface of the wall centered on the two head joints at the two third points. This system includes a primer, putty, saturant, and a glass fiber sheet to form the composite material. Glass fiber sheets were selected by the researchers in lieu of carbon FRP sheets based previous studies of retrofitting masonry systems by the research team. Glass fibers are more economical and provide a more compatible strength than the carbon fibers. The second method was the application of near surface mounted (NSM) glass FRP rods, illustrated in Figure 2.

Material and application material properties

The properties of the FRP rods and FRP fabric used in this study are detailed in Tables 2 and 3, respectively. Table 4 details the properties of the application materials. All material properties were evaluated using standard ASTM test methods. The mortar strength was 2000 psi, 1150 psi, and 1250 psi for Phase I-Series I, Phase I-Series II, and Phase II, respectively at test age of the walls. The compressive strength of the RC boundary elements was 4000 psi at test age. The concrete boundaries were one foot square beams, reinforced with three longitudinal #3 steel rebar top and bottom, allowing the beams to have the same strength in both directions. Shear reinforcement consisting of #3 stirrups spaced at 14 in (355.6 mm) on center were used in the boundary elements.

Phase I test set-up

Phase I tests were performed in the high-bay structural engineering laboratory at UMR. A strong wall was used as a reaction surface to load the URM walls. Concrete block was used to fill the void between the strong wall and the test location. RC beams, 12 in. (305 mm) square, were used as boundary elements on the top and bottom of the walls. The boundary members were post-tensioned to the strong floor as illustrated in Figure 3. The top member was also laterally restrained to the strong wall to limit translation at the top boundary. An air bag was placed between the test specimen and the concrete block fill to act as the loading mechanism. The bag was inflated incrementally and the pressure measured and recorded. As the bag inflated to a nominal level to bear against the wall, a strip along the edges of the wall was left unloaded. Dial gauges were used to measure the out-of-plane deflection (see Figure 3) and strain gauges were placed on the FRP to monitor the strain at each load increment where cracks were expected to form in the wall under out-of-plane load.

Phase II test set-up

The blast testing of the walls in Phase II took place at the United States Army Base at Fort Leonard Wood (FLW) near St. Roberts, Missouri. The tests were conducted on a certified military explosives range. The infill walls had boundary members (concrete beam / footing) on the top and bottom, respectively of the wall. A structural steel frame was designed to withstand the blast loading and support the boundary members and was anchored to the footings. The structural steel frame composed of 6 in × 6 in × 3/8 in (152 mm × 152 mm × 9.5 mm) tube sections and miscellaneous steel plates and angles is shown in Figure 4.

LABORATORY TEST RESULTS AND DISCUSSION

Of the twelve walls tested in this phase of the research program, none exhibited a shear problem or failure near the supports. When arching action is present, two possible failures can occur. The first is crushing of the masonry block and the second is the snapping through of the two rotating panels before crushing occurs. None of the walls showed signs of CMU crushing. The out-of-plane performance, development of arching action, and a description of the failure mode are provided for each wall.

Wall #1 -- Wall #1 was the first of the two unreinforced control walls. As testing began, an initial crack formed above the fourth course at 0.6 psi (4.1 kPa). Rotation, or the development of arching action, could be observed at the bottom of the wall. At 3.0

psi (20.7 kPa), a crack at the midspan joint occurred. After the crack occurred at midspan, a distinct development of arching action was observed just prior to failure (see Figure 5a, similar). Wall #1 failed at a pressure of 5.3 psi (36.5 kPa) with a deflection at failure of 1.3 in (33 mm).

Wall #2 -- Wall #2 was an unreinforced control with a shear retrofit. This wall performed much the same as Wall #1. Initial cracking was at the fourth course and occurred at 3.1 psi (21.4 kPa). Midspan cracking occurred at 4.0 psi (27.6 kPa) and development of arching action occurred (see Figure 5a, similar). Loading continued until failure with an ultimate load of 6.6 psi (45.5 kPa) and a deflection at failure of 0.74 in (18.8 mm).

Wall #3 -- Wall #3 was reinforced with 2.5 in (63.5 mm) wide sheets along the head joints. The sheets were anchored to the boundary members in this case. Initial cracking occurred at midspan at 3.1 psi (21.4 kPa), immediately followed by a crack above the fourth course at 3.2 psi (22.1 kPa). At 4.1 psi (28.3 kPa), a crack formed at the bottom course. Propagating cracks began to form at the intersection of the midspan crack and the GFRP sheet (similar Figure 5b). This was followed by the cracking of the block and additional propagation of cracks at midspan as well as above the fourth and fifth course. Distinct arching began to occur and a form of delamination was observed. The wall failed at 12 psi (82.7 kPa) with a deflection at failure of 1.5 in (38.1 mm). As the wall failed, pullout of the top anchorage occurred initially followed by the shearing of the sheets at the connection to the bottom boundary member. The rebar anchoring the sheets to the top member was broken near the location where the sheet was wrapped around it. The anchorage bar also pulled out of the top groove within the boundary element very clean, indicating that the bond between the rod and the paste may not have been good. The failure of the FRP can be classified as a delamination failure. However, there was no separation of the laminate from the wall. Concrete remained attached to the sheet after failure. The tensile strength of the concrete is reached before the bond breaks.

Wall #4 -- Wall #4 was also reinforced with 2.5 in. (63.5 mm) GFRP sheets. This wall had an ultimate capacity of 11.4 psi (78.6 kPa) and a maximum deflection of 1.1 in (27.9 mm). Midspan cracks formed at 3.4 psi (23.4 kPa) and a crack formed above the forth course at 3.8 psi (26.2 kPa). This wall also displayed the propagation of cracks as did the previous wall. Delamination was also present just prior to failure. Initially, the FRP ruptured at midspan, followed by shearing of the sheets at the bottom. There was a partial pullout at the top. One of the sheets pulled off the embedded rebar, while part of the other one stayed in tact. The top bar in this case also appeared to be pulling out fairly clean.

Wall #5 -- This wall was reinforced with two #2 GFRP bars along the head joints. The bars were anchored approximately three inches into the concrete boundary members. The failure occurred with the shearing of the FRP at three of the four connections. The fourth remained epoxied into the boundary member. Cracking began in this wall at 3.8 psi (26.2 kPa) with a midspan crack. Additional cracking continued with a crack above the fourth course at 4.4 psi (30.3 kPa). Several cracks formed through the blocks as shown in Figure 5b. Failure occurred at 10.2 psi (70.3 kPa) and a deflection of 1.2 in (30.5 mm).

Wall #6 -- The cracking of Wall #6 began at 2.6 psi (17.9 kPa) with a crack above the fourth course. This was followed by a midspan crack at 3.4 psi (23.4 kPa). During testing, the chain restraining translation of the top boundary broke. As a result, the pressure was decreased to a safe working level and the chain was replaced. Loading was then continued until failure was reached at a deflection of 1.1 in (27.9 mm) and a load of 11 psi (75.8 kPa). Failure occurred at midspan with the rupture of one of the FRP bars. The other bar pulled out of the bottom boundary, but remained attached at the top.

Wall #7 -- This was the first wall tested as part of Series II. This wall was reinforced with 2.5 in (63.5 mm) GFRP sheets that were not anchored to the concrete boundaries. An initial midspan crack occurred at 2.0 psi (13.8 kPa). At 2.4 psi (16.5 kPa), a crack formed above the fourth course. As was the case with the previous wall reinforced with sheets, propagating cracks began to form at midspan. Cracks illustrating the arching action can be seen in Figure 5a. Additional cracks formed through the blocks, as well as diagonal crack through the blocks visible from the side of the wall (Figure 5b). Delamination of the FRP accurred just prior to failure. A pressure of 9.6 psi (66.2 kPa) was achieved at a displacement of 1.8 in (45.7 mm). This wall test demonstrated the importance of anchoring the bonded laminates.

Wall #8 -- Wall #8 was reinforced with two unanchored #2 GFRP rebar. Initial cracks formed at midspan and above the fourth course. Propagation of cracks continued until failure at 4.8 psi (33.1 kPa), a load similar to the unreinforced condition. The deflection at failure was 0.96 in (24.4 kPa).

Wall #9 -- This wall was reinforced with NSM rods and made use of a running bond pattern, so the rods actually pass through some of the blocks. Cracking began above the fourth course at 2.2 psi (15.2 kPa) and at midspan at 3.0 psi (20.7 kPa). Extensive crack propagation was present, as were cracks through the blocks. Arching action was also clearly defined. 9.4 psi (64.8 kPa) was the failure load that occurred at 1.3 in (33.0 mm) of lateral displacement. The GFRP rods sheared off at the top, and one pulled out of the boundary at the bottom.

Wall #10 -- Wall #10 was reinforced with 2.5 in (63.5 mm) wide laminate strips anchored to the boundary. This wall was constructed using the running bond pattern. Initial cracking occurred above the fourth and fifth courses and at midspan at 1.8 psi (12.4 kPa). Propagating cracks began to occur at midspan and above the fourth course. Distinct arching action could be observed. The propagation of cracks continued with additional cracking through the blocks. Failure occurred at a pressure of 11.0 psi (75.8 kPa) and a displacement of 1.7 in (43.2 mm). Delamination was observed as were diagonal cracks through the 4 in (101.6 mm) dimension of the blocks. Pullout from the top beam occurred, but a portion of the rod remained in the beam. The FRP was sheared at the bottom boundary.

Wall #11 -- Wall #11 was reinforced with 4.5 in (111.8 mm) anchored FRP Sheets. This wall failed at a deflection of 1.9 in (48.3 mm) and a load of 12.6 psi (86.9 kPa). Cracking began at 2.0 psi (13.8 kPa) above the fourth course, followed by a crack at midspan at 2.8 psi (19.3 kPa). At 3.6 psi (24.8 kPa) there was a crack above the fifth course. Arching action and propagation of cracks were observed. There was also a shear crack through the block. Additional propagating cracks and cracks through the blocks

were observed. Extensive cracking occurred prior to the delamination failure at 12.6 psi (86.9 kPa). At the failure deflection of 1.9 in (48.3 mm), the FRP sheets pulled off of the bar anchoring them to the top boundary and sheared off at the bottom. The integrity of the wall system was generally intact after failure.

Wall #12 -- Wall #12 had the highest reinforcement ratio of all of the walls tested in Phase I. This wall was reinforced with 6.5 in (165.1 mm) wide sheets anchored to the boundaries. At 2.6 psi (17.9 kPa), cracks formed at midspan and above the fourth course. This was followed by additional cracking at 4.6 and 4.8 psi (31.7 and 33.1 kPa) above the fifth and second course, respectively. Initial failure was the pullout of the FRP sheets from the bottom beam followed by pullout from the top. This failure occurred at 15.2 psi (104.8 kPa) and a deflection of 1.9 in (48.3 mm). Arching and propagation cracks and cracks through the blocks were present. The laminates held the system intact after failure (Figure 5c).

ANALYSIS OF LABORATORY DATA AND FURTHER DISCUSSION

As the results indicate, strengthening the walls with FRP materials does in fact increase the wall's resistance to out-of-plane loads. Furthermore, the anchorage details allow for the development of continuity between the FRP and the concrete boundary elements. This can be seen by comparing the results of Walls #7 and #8 to Walls #3 through #6 as illustrated in Figure 6. Walls #3 through #6 investigate the condition in which the reinforcement is anchored to the boundary members. In Walls #7 and #8, the same reinforcement is used without the anchorage. For the case of the GFRP sheets, the unanchored condition provides a capacity between the unreinforced case and the anchored case. Some benefit can be obtained for walls with arching action just by applying the laminates to the walls. When anchorage of the sheets is provided, this research suggests additional capacity is gained. This is not true in the case of the NSM rods. When the NSM rods are installed without anchoring them to the boundary, they behave in much the same way as an unreinforced wall. When anchorage is provided, continuity is developed and additional capacity is obtained.

Walls #9 and #10 examined the effects of a URM wall's bond pattern on the strength increase provided by the FRP. These two walls were constructed using a running bond, so the FRP does not follow a continuous mortar joint. The FRP was anchored to the boundary element for this case. The walls performed similarly to those using the stacked bound used in the rest of the test program. Though not examined in this research, bond pattern may have an effect on the case where unanchored NSM rods are used. In this case, the rods would run through the face of the blocks in every other row. This may provide an increase in strength over the case of a stacked bond where the rod is placed in a continuous joint.

Walls #11 and #12 evaluated the influence of the width of the GFRP laminates on the out-of-plane strength. It is evident that as the width increases, the failure load also increases. As a rule, an increase in the strain energy, or area under the load deflection curve, usually provides a more desirable mode of failure. The load versus deflection curves for each wall are provided in Figure 7. As shown in this figure, two distinctly different initial stiffness values can be observed. The Series I walls have an increased stiffness over the walls from Series II. This is due to a variation in the compressive

strength of the mortar as reported previously. These two series of walls were constructed at different times, and as a result had different mortar compressive strengths even though their material compositions were similar. To allow for a more accurate comparison, a correction was performed. This was done by adjusting the deflections of the elastic portion of Series II walls. According to the Masonry Standards Joint Committee (2002), the mortar's modulus of elasticity is directly proportional to its compressive strength as shown in Equation 1. The measured deflections from Series II were corrected by multi-

$$E_g = 500 \times f_m^{'} \tag{1}$$

plying them by the ratio of their mortar strength to that of the walls in Series I. Essentially Series II walls were normalized based on the modulus of Series I walls. The deflections beyond the linear range (elastic wall response) were simply shifted the amount of the correction at the end of the linear range since the mortar had cracked and no longer contributed in a significant fashion to the stiffness of the wall system. The modified load versus deflection plot provides a more representative comparison for the two series of walls and is illustrated in Figure 8.

Using the plot of pressure versus modified deflection illustrated in Figure 8, the strain energy of each wall can be calculated by estimating the area under this load versus deformation curve. For this research, Wall #1 was used as a control or benchmark on which to base a strain energy ratio. The normalized strain energy as shown in Figure 9 is the ratio of the strain energy of a given wall to that of the control wall, Wall #1. From this figure, it is clear that the laminates provide the system with the ability to absorb more energy prior to failure. This was observed visually during the out-of-plane tests as well. The walls strengthened with NSM rods failed in a sudden brittle manner. When the laminates were used, more of the wall was intact, and impending failure was apparent by the large number and wide distribution of the crack patterns. Table 5 summarizes the initial failure modes for each wall and categorizes the failure as brittle or ductile based on their normalized strain energy ratio.

Two different methods were used to compare the ductility of the reinforcing techniques. The first method is the deflection ductility. This is calculated by dividing the wall's ultimate deflection (u_f) by its deflection at the apparent yield point (u_y). The second method is the energy ductility. This is determined by dividing the total area under the pressure versus corrected deflection plot by the area under the linear portion of the plot. Often, energy ductility is used to characterize and discuss the ductility of composite systems. Figure 10 shows both the normalized deflection and energy ductility based on the control wall, as well as for the walls strengthened with 2.5 in (63.5 mm) GFRP sheets and #2 NSM GFRP rods. For comparison, the ductility has been normalized with respect to the control wall. As illustrated in the figure based on two different ductility terms, strengthening the walls with both sheets and rods provides the wall system with additional ductility. Figure 11 illustrates the relationship between increasing laminate strip width and ductility. In this figure, the ductility ratio has been normalized with respect to the wall strengthened with 2.5 in (63.5 mm) wide sheets (the lowest reinforcement ratio). Again, the ductility increases as additional strengthening is provided. In the case of the sheets, as the ductility increased, the ability of the GFRP laminates to hold the wall together also increased. As shown in the results for Walls #11

and #12 (Figure 5c), the walls were largely held in tact as the amount of reinforcement and ductility increased.

The ability of the FRP to hold the wall together upon failure is important under blast loading. People can often survive a blast, but when hit by flying objects and debris, loss of life may occur. The pressures that would cause loss of life to a human are significantly higher than those that cause catastrophic damage to a building. If the integrity of walls in a building can be maintained, there is a reduced amount of flying debris that could potentially injure the occupants of the building. Increasing the amount of GFRP laminates on the wall was shown to improve the integrity of the wall system.

In several of the cases where the GFRP laminates were anchored to the boundaries, the GFRP rod used in the anchorage detail pulled out of the groove. Upon observation of the rod after failure, it was noted that little or no epoxy paste was still attached to the rod. This indicates that integrity of the system at higher reinforcement ratios is limited by the bond of the epoxy to the rod, and should be closely studied in future research.

To allow for the correlation of these results to those predicted theoretically, an equivalent uniform load was calculated. As the air bag inflates an area around the edges of the wall is left unloaded due to the size and shape of the air bag. To develop an expression for the equivalent uniform pressure, the load area and distribution was analyzed. The moment caused by loading the reduced area was first determined. The required pressure to cause this same moment given a uniform load over the entire wall was then calculated. It was determined that the equivalent uniform pressure was 66.3% of the pressure recorded during testing. Table 6 shows the equivalent uniform pressures for each wall. The relationship shown in Equation 2 developed by Shapiro et al. (1994) was then used to predict the capacity of an URM wall. This theory makes use of three coefficients, R_1, R2, and λ. R_1 is taken as 1.0 because there is no previous cracking. R_2 is taken as the minimum value of 0.5 because there is no framing along the sides of the wall. λ was taken as 0.0496, based on the wall's slenderness ratio. This model predicted an out-of-plane capacity of 5.58 psi (38.5 kPa) as shown below.

$$w = \frac{2f'_m}{h/t} R_1 R_2 \lambda \qquad (2)$$

h/t = 48/4 = 12 **f'$_m$** = 1350 psi **R_1** = 1 no previous cracking
λ = 0.0496 based on h/t **R_2** = 0.5 no framing on sides

$$w = \frac{2*1350}{12} * 1 * 0.5 * 0.0496 = 5.58 psi\ (38.5 kPa)$$

This value was slightly higher than the value causing failure of the test specimens in this research program. Based on the theoretical approach presented by Galati et al. (2003), the strength of the strengthened walls was predicted. The experimental and theoretical results are summarized in Table 7. Also listed in the table are the corresponding reinforcement indexes for each wall. These were determined as shown below using Equation 3.

$$\omega_f = \frac{\rho_f E_f}{f'_m (h/t_m)} \qquad (3)$$

For the 2.5 in laminates: E_f = 10500 ksi Thickness = 0.0139 in

Therefore:

$$\rho_f = \frac{A_f}{b_m t_m} = \frac{2.5*2*0.0139}{36*4} = 0.00024$$

$$w_f = \frac{0.00024*10500}{1.350*48/4} = 0.1556$$

Figure 12 plots the ratio of the experimental pressure to the theoretical pressure versus the reinforcement index. This plot indicates that the theoretical approach yields reasonable results in predicting the capacity of the walls. In the worst case, the experimental result was approximately 80% of the theoretical value. At times, conservative values result. The theoretical approach suggests that the crushing of the masonry is the primary mode of failure for most of the specimens. During testing, none of the walls failed due to masonry crushing; rather most of the failures were initiated by delamination of the strengthening technique. This may be due to the slight translation of the top boundary member during testing. This translation could have prevented the crushing of the masonry and allowed the wall to resist an increased load. Had rotation been fully restrained, concrete crushing may very well have controlled.

FIELD BLAST TEST RESULTS AND DISCUSSION

To verify the performance of the strengthening systems tested in the lab under blast loads, field blast tests were conducted on two walls. One of the walls was strengthened with GFRP laminates unanchored to the boundary elements, while the other made use of the same reinforcement but included the anchorage detail. Four damage levels have been established to categorize the damage caused by a blast load to test walls [Myers et al. (2002)]. Table 8 summarizes the blast loadings undertaken by the walls in this phase, as well as the level of damage the wall sustained under each loading.

Wall #1 -- Wall #1 was strengthened with 2.5 in (63.5 mm) GFRP laminates. No anchorage detail was provided for this wall to examine the differences in behavior of un-anchored and anchored walls. The wall survived the first blast event of 2 lb (0.9 kg) with minimal cracking sustaining light damage. The second blast event made use of 4 lb (1.8 kg) of pentolite explosive and caused a failure. Extensive cracking occurred in all of the mortar joints with a sliding failure of the mortar joint between the top course of blocks and the top boundary element where the wall was not anchored. Cracks formed through the blocks and a diagonal crack formed on the side of a mid-height block.

Wall #2 -- Wall #2 was strengthened with 2.5 in (63.5 mm) GFRP laminates that were anchored to the boundary members. This wall survived the first blast of 3 lb (1.4 kg) with light damage consisting of minimal cracking in some of the mortar joints. The following blast event induced heavy damage but did not result in failure of the wall system. Failure occurred when subjected to a 5 lb (2.3 kg) charge. Lateral rotation occurred with the loss of one of block form the wall, however, the anchorage details remained intact. Propagating cracks near the midspan mortar joint indicate that the wall system was approaching the onset of delamination.

The end stack of blocks comprising the wall began to rotate. It may be noted that in a continuous full scale wall, this rotation would not have occurred due to the fact that the column of blocks would have either been supported by a vertical boundary element or

bonded to the next column of blocks. There would not have been an end free to rotate as did the wall in this test program. Despite the rotation, the anchorage detail remained in tack, suggesting that addition capacity could have been obtained had the premature failure not occurred. Even with the rotation, the anchorage clearly provided an increase in capacity over the unanchored wall. The development of continuity between the FRP strengthening material and the surrounding boundary elements is key to increasing a walls out-of-plane strength and blast resistance for walls of similar slenderness ratios with arching action. Obviously this approach induces additional demands on the reinforced concrete frame and demands special attention to examine the overall system behavior of the framing system.

CONCLUSIONS

The objective of this research program was to evaluate the effectiveness of developing continuity between an FRP strengthened wall system and surrounding RC boundary elements. The effects of bond pattern and variable laminate strip width were also investigated. The conclusions drawn from this research are as follows:

- Additional capacity is gained by using all of the strengthening methods used in this research with exception to the case of unanchored NSM rods using a stacked bond. This reinforcement technique behaved much the same as the unreinforced wall.
- The development of continuity between the wall system and the surrounding frame provides additional capacity in the out-of-plane direction over the case where the strengthening material is not anchored to the boundary elements, both under static and blast testing.
- Bond pattern, stacked versus running, had limited effect on the out-of-plane strength of the walls.
- The laminate strips tend to hold the wall in tact as it fails, thereby reducing the scatter of debris under static out-of-plane testing. This reduces the risk to the inhabitants of the building.
- Increasing the width of the laminate strips provides additional capacity and allows the wall to fail as a unit, almost eliminating debris scatter under static out-of-plane testing. Laminates consisting of grid configurations may provide even a higher degree of limiting debris scatter.
- The bond characteristics of the various pastes used to apply NSM rods needs to be further investigated to properly evaluate the true strength of the anchorage details.
- The field blast test dynamically validate the laboratory results which suggest that the use of anchorage details or the development of continuity between the wall system and the surrounding RC frame provide additional capacity in the out-of-plane direction beyond that gained by strengthening alone.

ACKNOWLEDGEMENTS

The authors would to acknowledge the NSF/Industry sponsored Repair of Buildings and Bridges with Composites Cooperative Research Center (RB2C) at the University of Missouri-Rolla (USA) for supporting this research study.

REFERENCES

Angel, R., Abrams, D. P., Shapiro, D., Uzarski, J., and Webster, M. (1994). "Behavior of Reinforced Concrete Frames with Masonry Infills." Structural Research Series No. 589, Department of Civil Engineering, Univeristy of Illinois at Urbana-Champaign, IL.

El-Domiaty, K. A., Myers, J. J., Belarbi, A. (2002). "Blast Resistance of Un-Reinforced Masonry Walls Retrofitted with Fiber Reinforced Polymers." Center for Infrastructure Engineering Studies Report 02-28, University of Missouri – Rolla, Rolla, MO.

Galati, N., Tumialan, J. G., and Nanni, A. (2003) "Influence of Arching Mechanism in Masonry Walls Strengthened With FRP Laminates." Submitted to ACI International, January, 2003.

Hughes Brothers, Inc. (2001) "Glass Fiber Reinforced Polymer (GFRP) Rebar, Aslan 100." Seward, NE.

Masonry Standard Joint Committee (2002). "Building Code Requirements for Masonry Structures," ACI 530-02/ASCE 5-02/TMS 402-02. American Concrete Institute, American Society of Civil Engineers, and The Masonry Society, Farmington Hills, MI, Reston, VA, Boulder, CO.

Mays, G.C. and Smith, P.D. (1995) Blast Effects on Buildings. Thomas Telford, London.

Myers, J. J., Belarbi, A. El-Domiaty, K. A., "Blast Resistance of Un-reinforced Masonry Walls Retrofitted with Fiber Reinforced Polymers," The Masonry Society Journal, Boulder, Colorado, Vol.22, No.1, September 2004, pp. 9-26.

Shapiro, D., Uzarski, J., Webster, M., Angel, R., and Abrams, D. (1994). "Estimating Out-of-Plane Strength of Cracked Masonry Infills." Report, Department of Civil Engineering, University of Illinois, Urbanna, IL sponsored by the National Science Foundation, Arlington, VA.

Watson Bowman Acme Corp. (2002a). "Wabo®MBrace Composite Strengthening System, Engineering Design Guidelines." Amherst, NY.

Watson Bowman Acme Corp. (2002b). "Wabo®MBrace EG900, Unidirectional E-Glass Fiber Fabric." Amherst, NY.

Table 1 -- Experimental Test Matrix

Walls			Retrofit Scheme					
			FRP Sheets	Sheet Width	NSM FRP Rods	Anchor-age	Stacked Bond	Running Bond
Phase I	Series I	#1					√	
		#2					√	
		#3	√	2.5"		√	√	
		#4	√	2.5"		√	√	
		#5			√	√	√	
		#6			√	√	√	
	Series II	#7	√	2.5"			√	
		#8			√		√	
		#9			√	√		√
		#10	√	2.5"		√		√
		#11	√	4.5"		√	√	
		#12	√	6.5"		√	√	
Phase II		#1	√	2.5"			√	
		#2	√	2.5"		√	√	

Conversion: 1in = 25.4 mm Key: √ - includes detail

Table 2 -- Properties of GFRP Rebar (Hughes 2001)

Bar Size	Cross Sectional Area (in^2)	Nominal Diameter (in)	Tensile Strength (ksi)	Tensile Modulus of Elasticity (ksi)
#2	0.0515	0.25	120	5920

Conversions: 1 in = 25.4 mm, 1 in^2 = 645.2 mm^2, 1 ksi = 6.895 MPa

Table 3 -- Properties of GFRP Fabric (Watson 2002b)

Nominal Thickness (in)	Ultimate Tensile Strength (ksi)	Tensile Modulus of Elasticity (ksi)	Ultimate Rupture Strain	Ultimate Tensile Strength per Unit Width (k/in)
0.0139	220	10500	2.1%	3.06

Conversions: 1 in = 25.4 mm, 1 ksi = 6.895 MPa, 1 k/in = .175 kN/mm

Table 4 -- Properties of Application Materials ([1]Watson 2002a, [2]ChemRex® 2002)

	Primer[1]	Putty[1]	Saturant[1]	Paste[2]
Tensile Strength (psi)	2500	2200	8000	4000
Tensile Strain	0.40	0.06	0.03	0.01
Tensile Modulus (psi)	104,000	260,000	440,000	-
Poisson's Ratio	0.48	0.48	0.40	-
Compressive Strength (psi)	4100	3300	12,500	12,500
Compressive Strain	0.10	0.10	0.05	-
Compressive Modulus (psi)	97,000	156,000	380,000	450,000

Conversion: 1 psi = 6.895 kPa

Table 5 -- Summary of Failure Modes for Phase I

Wall	Initial Failure Mode	Brittle / Ductile
1	Bed Joint Failure	Brittle
2	Bed Joint Failure	Brittle
3	Delamination	Ductile
4	Delamination / FRP Rupture	Neutral
5	FRP Shear at Connections	Brittle
6	FRP Rupture	Neutral
7	Delamination	Ductile
8	Bed Joint Failure	Brittle
9	FRP Shear and Pullout at Connections	Neutral
10	Delamination	Ductile
11	Delamination	Ductile
12	Connection Pullout	Ductile

Table 6 -- Equivalent Uniform Pressures

Wall #	Experimental Pressure (psi)	Equivalent Uniform Pressure (psi)
1	5.3	3.5
2	6.6	4.4
3	12.0	8.0
4	11.4	7.6
5	10.2	6.8
6	11.0	7.3
7	9.6	6.4
8	4.8	3.2
9	9.4	6.2
10	11.0	7.3
11	12.6	8.4
12	15.2	10.1

Table 7 -- Experimental and Theoretical Results

Wall #	Experimental Pressure (psi)	Theoretical Pressure (psi)	Reinforcement Index (ω_f)
1	3.5	3.7	-
2	4.4	3.7	-
3	8.0	6.75	0.1556
4	7.6	6.75	0.1556
5	6.8	6.46	0.2631
6	7.3	6.46	0.2631
7	6.4	5.3	0.1556
8	3.2	3.9	0.2631
9	6.2	6.46	0.2631
10	7.3	6.75	0.1556
11	8.4	7.4	0.2787
12	10.1	7.85	0.4083

Conversion: 1 psi = 6.895 kPa

Table 8 -- Summary of Blast Events and Levels of Failure

Wall	Charge Weight (lb)	Standoff Distance (ft)	Level of Damage
Wall #1	2	6	Light Damage
	4	6	Failure
Wall #2	3	6	Light Damage
	4	6	Heavy Damage
	5	6	Failure

Conversions: 1 ft = 12 in =25.4 mm, 1 lb = 0.45 kg

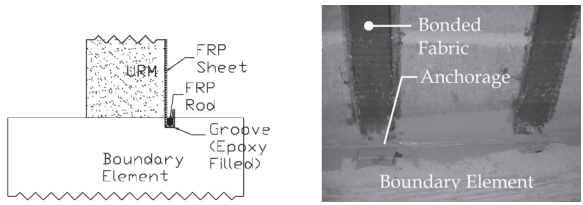

Figure 1 — FRP Laminate Detail

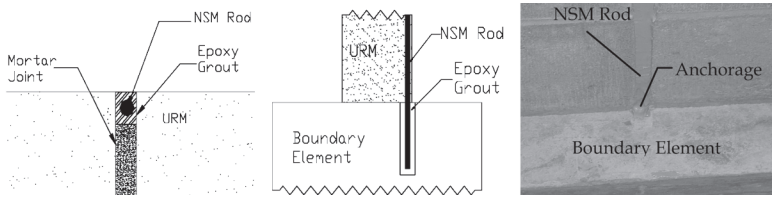

Figure 2 — NSM FRP Rod Detail

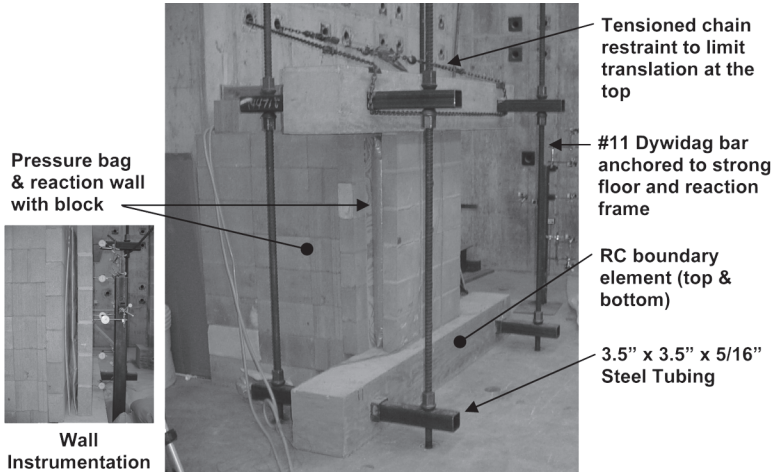

Figure 3 — Phase I Test Setup and Instrumentation (Laboratory)

Figure 4 — Phase II Test Set-up with Suspension of Charge (Field)

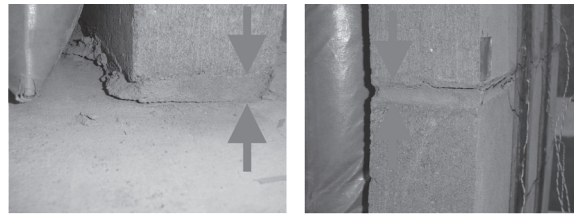

a) Formation of Arching Action: Base of Wall, Mid-height of Wall

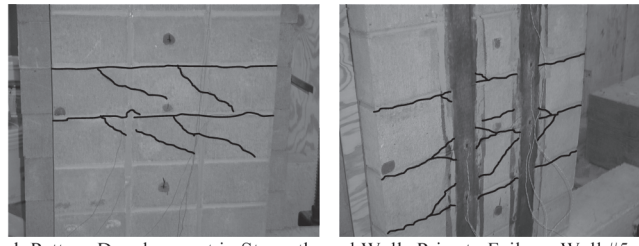

b) Crack Pattern Development in Strengthened Walls Prior to Failure: Wall #5, Wall #7

c) Debris Scatter: URM (Wall#2), NSM GRFP (Wall #8), Bonded Fabric (Wall #12)

Figure 5 — Wall Behavior of Various Systems as Noted

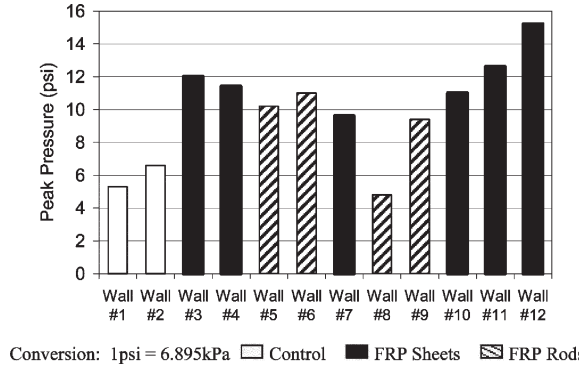

Figure 6 — Peak Out-of-Plane Pressure Results for Phase I Test Walls at Failure

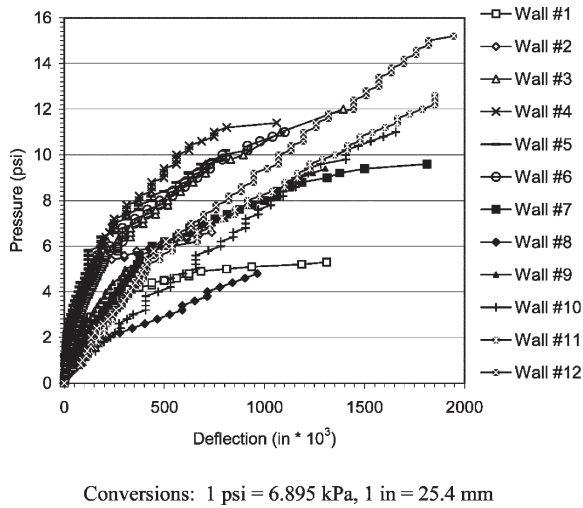

Figure 7 — Pressure versus Displacement for Phase I Walls

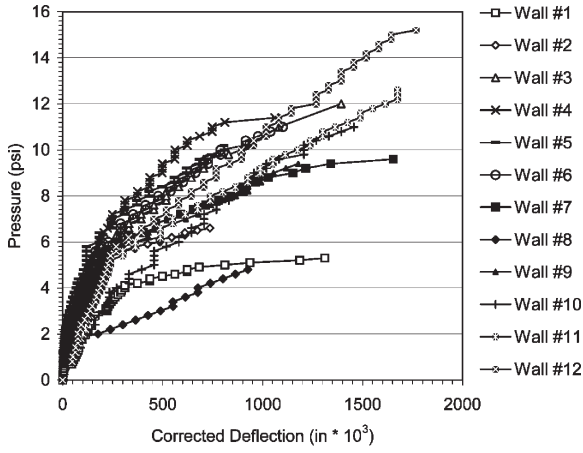

Conversions: 1 psi = 6.895 kPa, 1 in = 25.4 mm

Figure 8 — Pressure versus Modified Displacement

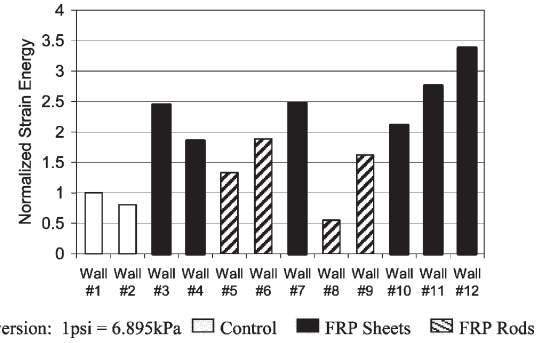

Figure 9 — Normalized Strain Energy Ratio

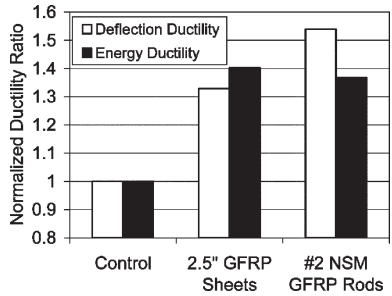

Figure 10 — Strengthening Scheme Effects on Normalized Ductility Ratio

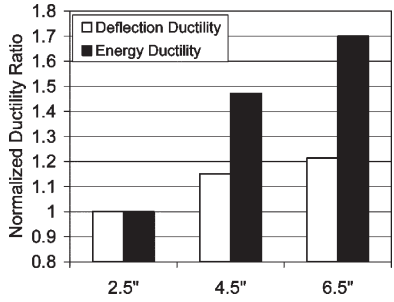

Figure 11 — Laminate Strip Width Effects on Normalized Ductility Ratio

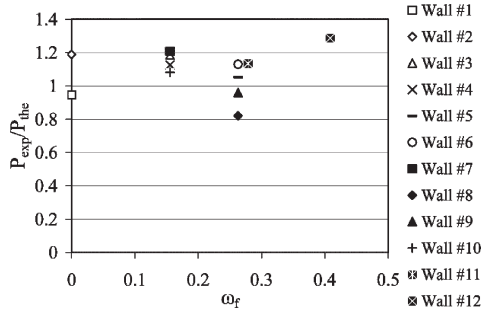

Figure 12 — Pressure Ratio versus Reinforcement Index